

On the crystal structures and hydrogen bond patterns in proline pseudopolymorphs

Luis E. Seijas, Gerzon E. Delgado,^{a)} and Asiloé J. Mora^{a)}

Laboratorio de Cristalografía, Departamento de Química, Facultad de Ciencias, Universidad de Los Andes, Mérida 5101, Venezuela

Andrew N. Fitch

European Synchrotron Radiation Facility, BP220, F-38043 Grenoble Cedex, France

Michela Brunelli

Institut Laue Langevin, BP156, F-38042 Grenoble Cedex, France

(Received 7 May 2010; accepted 7 July 2010)

Amino acids often cocrystallize with water molecules, which make them pseudopolymorphs of their anhydrous forms. In this work, we discuss in detail the hydrogen bond patterns in anhydrous L-proline and DL-proline and its pseudopolymorphic forms: L-proline monohydrate and DL-proline monohydrate. For this propose, the crystal structure of L-proline anhydrous was determined from synchrotron X-ray powder diffraction data and refined using the Rietveld method. Special emphasis is given to the role played by the water molecule in the hydrogen bond network observed in the crystalline structures. © 2010 International Centre for Diffraction Data. [DOI: 10.1154/1.3478557]

Key words: hydrogen bonding, proline, pseudopolymorphs, crystal structure, X-ray powder diffraction, synchrotron radiation

I. INTRODUCTION

Among the 20 natural amino acids, L-proline [2*S*-pyrrolidin-2-carboxylic acid (Figure 1)] is the only one having a secondary amino group in the form of a pyrrolidinic ring, which gives interesting structural characteristics whenever this amino acid is present. For instance, the presence of an L-proline fragment in a protein splits α helices due to structural restrictions imposed by the pyrrolidine ring. In general, L-proline is found in the regions where β turns exist, and therefore it can be located in the surface of a protein (Voet and Voet, 1995). The structure of polyproline is highly directional and composed of three left hand helices similar to the helices of collagen (Burge *et al.*, 1962). From the point of view of its capability for H bonding, proline is only allowed to donate two hydrogen atoms to form H bonds; on the other hand, the carboxylate moiety is able to accept at least four hydrogen atoms to form H bonds. A way to compensate this imbalance situation is the formation of water adducts with the amino acid, in which each water molecule adds two hydrogen atoms for H bonding.

A search in the Cambridge Structural Database (Allen, 2002) shows four reports of proline: L-proline anhydrous (PROLIN; $R=16.9\%$) (Kayushina and Vainshtein, 1965), L-proline monohydrate (RUWGEV; $R=3.3\%$) (Janczak and Luger, 1997), DL-proline anhydrous (QANRUT; $R=4.0\%$) (Myung *et al.*, 2005), and DL-proline monohydrate (DL-PROM01; $R=3.9\%$) (Padmanabhan *et al.*, 1995); (DL-PROM02; $R=2.1\%$) (Flaig *et al.*, 2002). The hydrated forms are considered pseudopolymorphic forms of the anhydrous amino acids (Yin and Li, 2006; Nangia and Desiraju, 1999). L-proline anhydrous (PROLIN) was investigated using pho-

tographic data of low resolution, which did not afforded structural details concerning hydrogen bonds (Kayushina and Vainshtein, 1965).

The aim of this work is to report the structure of L-proline characterized from X-ray synchrotron powder diffraction data to provide information on crystal packing and H bonds. Furthermore, a detailed discussion of the crystal packings of optically pure proline and racemic pseudopolymorphs is presented, particularly assessing hydrogen bonds and the van der Waals interactions.

II. EXPERIMENTAL

A. Synchrotron X-ray powder diffraction

The X-ray powder diffraction data were collected on the high-resolution powder X-ray diffractometer of beamline ID31 at ESRF (Fitch, 2004) with a wavelength of 1.252 54 (3) Å. Small quantities of L-proline at 99% purity (obtained from commercial source, ALDRICH) were loaded at room temperature into a 1.5 mm diameter borosilicate thin walled glass capillary, spun at approximately 1 Hz, during

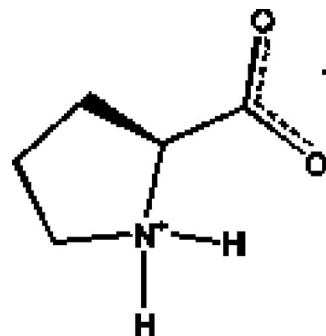


Figure 1. Diagram of the amino acid proline.

^{a)} Authors to whom correspondence should be addressed. Electronic addresses: gerzon@ula.ve and asiloe@ula.ve

measurements. The data were collected for several hours and normalized against monitor counts and detector efficiencies and rebinned into steps of $2\theta=0.003^\circ$.

B. Structure determination and refinement

The diffraction pattern of the L-proline was indexed in an orthorhombic cell with $a=11.6877(4)$ Å, $b=9.0685(3)$ Å, and $c=5.2697(2)$ Å using the program DICVOL04 (Boultif and Louër, 2004), with figures of merit: $M_{(20)}=348.5$ (de Wolff, 1968) and $F_{(20)}=739.9$ (0.001, 28) (Smith and Snyder, 1979). Evaluation of the systematic absences in the diffraction pattern indicated the space group $P2_12_12_1$ (No. 19). The pattern decomposition was made using the Le Bail method (Le Bail *et al.*, 1988) and the crystal structural solution was obtained by direct methods using the program EXPO2009 (Altomare *et al.*, 2009). All eight non-hydrogen atoms from the molecule were found in the E map of the best solution proposed by the EXPO2009 program. The hydrogen atoms were placed in calculated positions with restricted geometries using the HFIX command of the program SHELXL (Sheldrick, 2008). The model was refined by the Rietveld method (Rietveld, 1969) using the program GSAS (Larson and Von Dreele, 2004). The data were restrained to the 2θ range of 5° to 65° , comprising 252 Bragg reflections, which were modeled using a pseudo-Voigt peak shape function (Thompson *et al.*, 1987), with the inclusion of the axial divergence asymmetry correction at low angle (Finger *et al.*, 1994).

The background was fitted by the automatic interpolation of 20 points through the whole pattern. Bond distances and angle restraints were applied using the average values obtained from structures contained the pyrrolidinic ring found in the CSD (Allen, 2002) and the three pseudopolymorphs of the proline previously reported (RUWGEV, QANRUT, and DLPROM02). Bond distances and angle restraints were weighted, 0.05 Å and 1° , respectively. H atoms were refined with C-H and N-H distances restrained to be 0.970 and 0.900, respectively (weighted 0.02 Å). The isotropic displacement parameters for all H atoms were constrained to be $1.5U_{\text{iso}}$ (parent). Table I shows experimental details for the data collection, the structural solution, and the Rietveld refinement. The final Rietveld plot is shown in Figure 2.

III. RESULTS AND DISCUSSION

The pyrrolidinic ring presents different conformations in the different compounds. For RUWGEV, QANRUT, and DLPROM02 the closest pucker descriptor is twisted in $C^\gamma-C^\delta$, $C^\alpha-C^\beta$, and $C^\beta-C^\gamma$, respectively, and envelop on C^β for the L-proline. The carboxylate group in the crystalline structures of RUWGEV and DLPROM02 has a bisectonal orientation forming angles with the Cremer and Pople normal plane (Cremer and Pople, 1975) of $37.2(3)^\circ$ and $35.6(1)^\circ$, while the structures QANRUT and L-proline have an axial orientation with angles of $9.2(1)^\circ$ and 15.3° , respectively.

TABLE I. Crystal and experimental data.

Parameter	Values
Empirical formula	$C_5H_9NO_2$
Formula weight	115.13
Crystal system	Orthorhombic
Space group	$P2_12_12_1$
Unit cell dimensions	$a=11.688\ 43(4)$ Å, $b=9.068\ 32(3)$ Å, $c=5.270\ 13(1)$ Å
V	$558.605(4)$ Å ³
Z	4
D_{cal}	$1.369\ \text{g/cm}^3$
Radiation (synchrotron)	$1.252\ 54$ Å
Range for data collection	5° to 65.92°
Temperature	295 K
No. of parameters	87
Figures of merit (R_p, R_{wp}, χ^2)	0.089, 0.139, 2.43
Refinement method	Rietveld
Measurement	Beamline ID31, ESRF
Structure determination/refinement	EXPO2009/GSAS
Molecular graphics	DIAMOND

The calculated densities of the parents DL-proline: L-proline and DL-proline monohydrate: L-proline monohydrate (Table II) indicate that these compounds are a typical example of one that follows Wallach's rule (Wallach, 1895), which states that racemic crystals tend to be denser than their chiral counterparts.

The four proline structures crystallize in different space groups (see Table II), and they can be placed in two categories: (i) enantiomeric, in which the hydrogen bonds occur around a screw axis and (ii) racemic crystals, in which the hydrogen bonds link molecules related by mirror planes or inversion centers (Dalhus and Görbitz, 2004). The four proline crystalline structures are stabilized by hydrogen bonds and the van der Waals interactions, and geometry parameters of the hydrogen bonds are summarized in Table III.

The crystalline structure of L-proline is stabilized by two intermolecular hydrogen bonds, which involve the carboxylate and amino groups in a set of head-to-tail interactions, as is shown in Figure 3(a). The $N1-H1\cdots O2$ ($1-x, -\frac{1}{2}+y, \frac{1}{2}-z$) hydrogen bond forms molecular chains along the b axis,

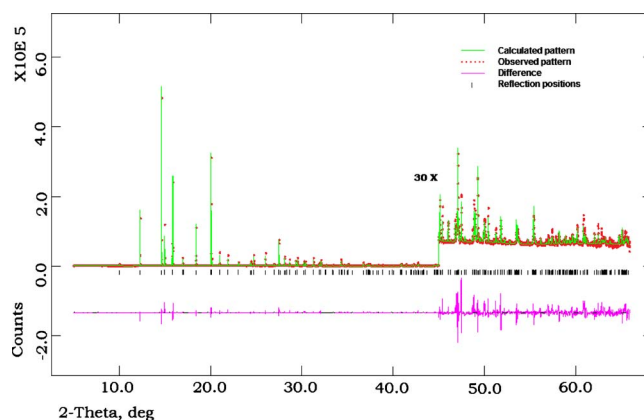


Figure 2. (Color online) Final Rietveld plot for the refinement of the L-proline at room temperature.

TABLE II. Crystal data for the pseudopolymorphs of the proline.

	L-proline (this work)	L-proline monohydrate (RUWGEV)	DL-proline (QANRUT)	DL-proline monohydrate (DLPROM02)
Space group	$P2_12_12_1$ (No. 19)	$C2$ (No. 5)	$P2_1/c$ (No. 14)	$Pbca$ (No. 61)
Z (Z')	4(1)	4(1)	4(1)	8(1)
T (K)	295	100	120	100
D_{cal} (g/cm^3)	1.369	1.368	1.409	1.414
Unit cell parameters (\AA , deg)	$a=11.688\ 43(4)$ $b=9.068\ 32(3)$ $c=5.270\ 13(1)$	$a=20.431(4)$ $b=6.192(1)$ $c=5.136(1)$ $\beta=95.79(2)$	$a=8.9906(6)$ $b=5.2987(4)$ $c=11.4786(8)$ $\beta=97.041(2)$	$a=5.253(3)$ $b=11.987(5)$ $c=19.864(1)$
Volume (\AA^3)	558.6(1)	646.4(2)	542.70(7)	1250.8(9)

with graph set $C(5)$ (Etter, 1990) and the $\text{N1-H2}\cdots\text{O1}$ ($x, y, -1+z$) hydrogen bond links these chains forming another one, with the same graph set $C(5)$. The crossing of these two chains causes the formation of a macrocycle with second order graph set $R_4^4(16)$. The proline molecules stack along a forming molecular layer, where it is possible to observe hydrophilic and hydrophobic regions [see Figure 3(b)]. All crystal structure diagrams were performed using DIAMOND (Bergerhoff *et al.*, 1996).

Figure 4(a) shows a partial packing view of RUWGEV, L-proline monohydrate, where it can be observed the interactions between amino and carboxylate groups through the hydrogen bonds $\text{N1-H1}\cdots\text{O1}$, $\text{N1-H1}\cdots\text{O2}$ ($\frac{1}{2}-x, \frac{1}{2}+y, 1-z$), and $\text{N1-H2}\cdots\text{O1}$ ($x, y, -1+z$) where the H1 atom acts as a bifurcated donor forming part of two hydrogen bonds with graph set $R_4^2(4)$ [see Figures 4(a) and 4(b)]. These hydrogen bonds link the L-proline molecules in order to form pairs of chains in opposite directions, running along c , which are related by twofold screw axes. The ribbons of L-proline

are interconnected through the hydrogen bonds $\text{O3-H11}\cdots\text{O2}$ ($1-x, -1+y, 2-z$), $\text{N1-H1}\cdots\text{O1}$ ($\frac{1}{2}-x, \frac{1}{2}+y, 1-z$), and $\text{N1-H1}\cdots\text{O2}$ ($\frac{1}{2}-x, \frac{1}{2}+y, 1-z$), which are described by the graph set $C_4^4(11)\{R_1^2(4)\}$. The water molecules are related by a twofold axis and form zigzag chains of $\text{O-H}\cdots\text{O}$ hydrogen bonds parallel to the c axis, described by the graph set $C_2^2(4)$; this chain stabilizes the crystalline structure by cooperative effects on the hydrogen bonding. Figure 4(b) shows as columns of molecules stack in layers parallel to the ac plane and channels of water molecules along c . Comparing this structure with the previous one, it can be noticed that inclusion of the water molecule into the crystal lattice induces changes in the hydrogen bond patterns, made apparent in the formation a bifurcated donor hydrogen bond capable of saturating the acceptor capacity of O1 of the carboxylate group while O2 accepts a hydrogen bond from the water molecule.

TABLE III. Hydrogen bonding geometry of the four pseudopolymorphs (\AA , deg).

Compound	D-H \cdots A	D-H	H \cdots A	D \cdots A	D-H \cdots A
L-proline (this work)	$\text{N1-H1}\cdots\text{O2}$ ^a	0.900(5)	2.384(5)	3.195(5)	150.0(4)
	$\text{N1-H2}\cdots\text{O1}$ ^b	0.900(5)	1.841(4)	2.723(4)	165.7(5)
L-proline monohydrate (RUWGEV)	$\text{N1-H1}\cdots\text{O1}$ ^c	0.900(5)	2.581(5)	3.243(5)	130.9(4)
	$\text{N1-H1}\cdots\text{O2}$ ^c	0.900(5)	2.384(5)	3.195(5)	150.0(4)
	$\text{N1-H2}\cdots\text{O1}$ ^b	0.900(5)	1.841(4)	2.723(4)	165.7(5)
	$\text{O3-H11}\cdots\text{O3}$ ^d	0.8900	2.1600	2.889(4)	139.00
	$\text{O3-H12}\cdots\text{O3}$ ^e	0.9000	2.0300	2.902(4)	161.00
DL-proline (QANRUT)	$\text{N1-H1}\cdots\text{O1}$ ^f	0.900(5)	2.384(5)	3.195(5)	150.0(4)
	$\text{N1-H2}\cdots\text{O1}$ ^g	0.900(5)	1.841(4)	2.723(4)	165.7(5)
DL-proline monohydrate (DLPROM02)	$\text{N1-H1}\cdots\text{O1}$ ^h	0.920(2)	1.800(2)	2.713(1)	171.8(2)
	$\text{N1-H2}\cdots\text{O2}$ ⁱ	0.906(2)	2.093(2)	2.839(2)	138.9(2)
	$\text{O3-H10}\cdots\text{O2}$ ^j	0.856(1)	2.222(9)	2.8520(18)	163.9(1)
	$\text{O3-H11}\cdots\text{O3}$ ^k	0.857(1)	1.900(10)	2.7344(16)	163.9(1)

^a $1-x, -\frac{1}{2}+y, \frac{1}{2}-z.$

^b $x, y, -1+z.$

^c $\frac{1}{2}-x, \frac{1}{2}+y, 1-z.$

^d $1-x, -1+y, 2-z.$

^e $1-x, y, 1-z.$

^f $x, -1+y, z.$

^g $-x, 1-y, -z.$

^h $x, 1-y, -z.$

ⁱ $1+x, y, z.$

^j $\frac{1}{2}-x, -\frac{1}{2}+y, z.$

^k $\frac{1}{2}+x, y, \frac{1}{2}-z.$

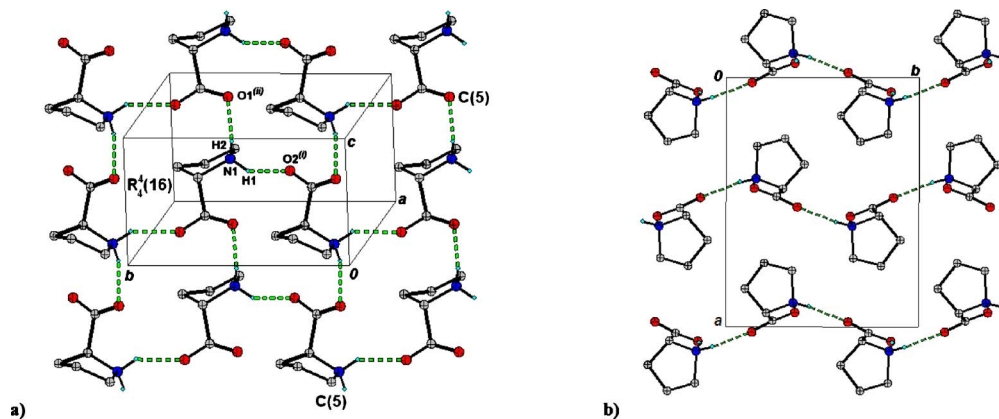


Figure 3. (Color online) (a) Partial packing view and (b) view along the *c* axis of L-proline. Broken lines indicate hydrogen bonds. H atoms not involved in hydrogen bonding have been omitted for clarity.

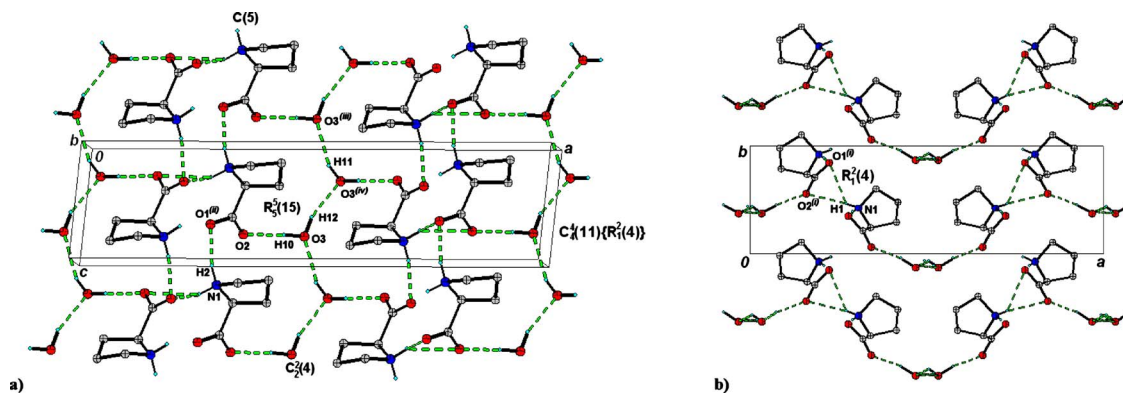


Figure 4. (Color online) (a) Partial packing view and (b) view along the *c* axis of L-proline·H₂O.

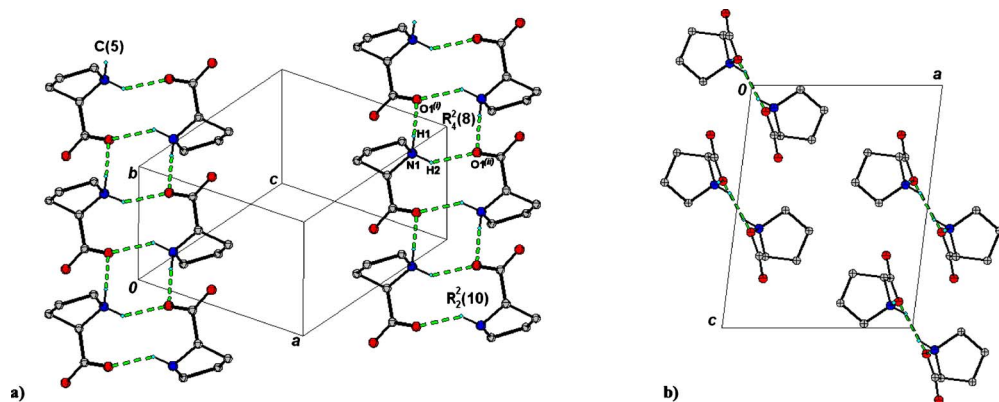


Figure 5. (Color online) (a) Partial packing view and (b) view along the *b* axis of DL-proline.

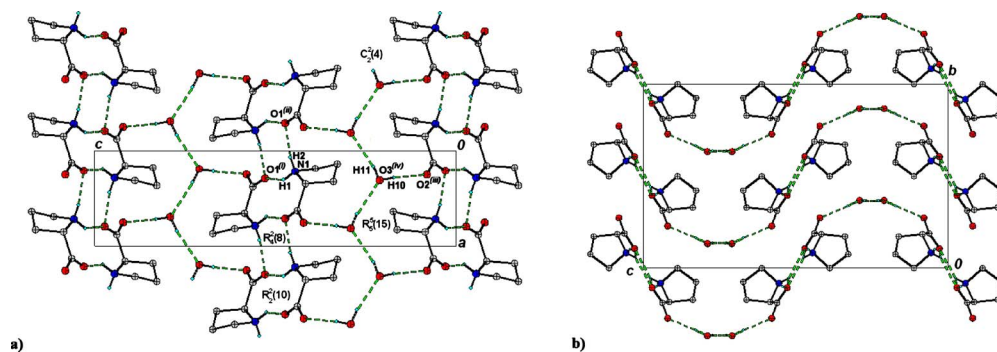


Figure 6. (Color online) (a) Partial packing view and (b) view along the b axis of DL-proline H_2O .

The crystalline structure of QANTRUT (DL-proline) is stabilized by two hydrogen bonds, which involve the carboxylate and the ammonium groups. The hydrogen bond $\text{N1-H1}\cdots\text{O1}$ ($x, -1+y, z$) forms chains parallel to (-101) , which can be described by the graph set $\text{C}(5)$. These chains are connected between them by $\text{N1-H2}\cdots\text{O1}$ ($-x, 1-y, -z$), making the O1 atom a bifurcated acceptor, forming rings with graph sets $\text{R}_4^2(8)$ and $\text{R}_2^2(10)$ [Figure 5(a)]. Figure 5(b) shows the hydrophilic and hydrophobic regions clearly defined. In the center of the cell the hydrophobic CH_2 from the pyrrolidine ring interacts through the van der Waals forces.

Figure 6(a) shows a partial packing view of DLPROM02 (DL-proline monohydrate), which resembles the anhydrous form (QANTRUT). The $\text{N1-H1}\cdots\text{O1}$ ($x, 1-y, -z$) and $\text{N1-H2}\cdots\text{O2}$ ($1+x, y, z$) hydrogen bonds induce the formation of molecular ribbons in a set of head-to-tail interactions of the proline molecules. Water molecules related by the c glide plane occur in infinite channels along a forming a chain, with the hydrogen bonds $\text{O3-H10}\cdots\text{O2}$ ($\frac{1}{2}-x, -\frac{1}{2}+y, z$) and $\text{O3-H11}\cdots\text{O3}$ ($\frac{1}{2}+x, y, \frac{1}{2}-z$), which are described by the graph set $\text{C}_2^2(4)$. The formation of rings with graph sets $\text{R}_4^2(8)$, $\text{R}_2^2(10)$, and $\text{R}_5^2(15)$ is also observed. These molecules interconnect the proline ribbons by a short chain of $\text{O-H}\cdots\text{O}$ hydrogen bonds [Figure 6(a)] to form undulated layers parallel to the ac plane. These layers stack along the b axis [Figure 6(b)].

IV. CONCLUSION

The four pseudopolymorphs of proline are stabilized by hydrogen bonds where the head-to-tail interactions between adjacent molecules are dominant and produce stacks of molecular ribbons made up from chains of molecules pointing in opposite directions. This is an evidence of the high stability of this type of superstructure based on hydrogen bonds. Furthermore, all the pseudopolymorph structures display layered packings stabilized by the van der Waals interactions.

ACKNOWLEDGMENTS

This work was supported by CDCHT-ULA (Grant Nos. C-1618-08-AA and C-1619-08-Ed), FONACIT (Grant No. LAB-97000821), and ESRF (Grant No. CH-2490).

Allen, F. H. (2002). "The Cambridge Structural Database: A quarter of a million crystal structures and rising." *Acta Crystallogr., Sect. B: Struct.*

Sci. **58**, 380–388.

- Altomare, A., Camalli, M., Cuocci, C., Giacovazzo, C., Moliterni, A., and Rizzi, R. (2009). "EXPO2009: Structure solution by powder data in direct and reciprocal space." *J. Appl. Crystallogr.* **42**, 1197–1202.
- Bergerhoff, G., Berndt, M., and Brandenburg, K. (1996). "Evaluation of crystallographic data with the program DIAMOND." *J. Res. Natl. Inst. Stand. Technol.* **101**, 221–225.
- Boutlif, A. and Louër, D. (2004). "Powder pattern indexing with the dichotomy method." *J. Appl. Crystallogr.* **37**, 724–731.
- Burge, R. E., Harrison, P., and McGavin, S. (1962). "The structure of the poly-L-proline II." *Acta Crystallogr.* **15**, 914–915.
- Cremer, D. and Pople, J. A. (1975). "General definition of ring puckering coordinates." *J. Am. Chem. Soc.* **97**, 1354–1358.
- Dalhus, B. and Görbitz, C. H. (2004). "Crystal structures of hydrophobic amino acids: Interaction energies of hydrogen-bonded layers revealed by ab initio calculations." *J. Mol. Struct.: THEOCHEM* **675**, 47–52.
- de Wolff, P. M. (1968). "A simplified criterion for the reliability of a powder pattern indexing." *J. Appl. Crystallogr.* **1**, 108–113.
- Etter, M. C. (1990). "Encoding and decoding hydrogen-bond patterns of organic-compounds." *Acc. Chem. Res.* **23**, 120–126.
- Finger, L. W., Cox, L. W., and Jephcoat, A. P. (1994). "A correction for powder diffraction peak asymmetry due to axial divergence." *J. Appl. Crystallogr.* **27**, 892–900.
- Fitch, A. N. (2004). "The high resolution powder diffraction beam line at ESRF." *J. Res. Natl. Inst. Stand. Technol.* **109**, 133–142.
- Flaig, R., Koritsanszky, T., Dittrich, B., Wagner, A., and Luger, P. (2002). "Intra- and intermolecular topological properties of amino acids: A comparative study of experimental and theoretical results." *J. Am. Chem. Soc.* **124**, 3407–3417.
- Janczak, J. and Luger, P. (1997). "L-proline monohydrate at 100 K." *Acta Crystallogr., Sect. C: Cryst. Struct. Commun.* **53**, 1954–1956.
- Kayushina, R. L. and Vainshtein, B. K. (1965). "X-ray determination of the structure of L-proline." *Kristallografiya* **10**, 833–844.
- Larson, A. C. and Von Dreele, R. B. (2004). *General Structure Analysis System (GSAS)*, Report LAUR 86-748, Los Alamos National Laboratory, Los Alamos, NM.
- Le Bail, A., Duroy, H., and Fourquet, J. L. (1988). "Ab-initio structure determination of LiSbWO_6 by X-ray-powder diffraction." *Mater. Res. Bull.* **23**, 447–452.
- Myung, S., Pink, M., Baik, M.-H., and Clemmer, D. E. (2005). "DL-proline." *Acta Crystallogr., Sect. C: Cryst. Struct. Commun.* **61**, 506–508.
- Nangia, A. and Desiraju, G. R. (1999). "Pseudopolymorphism: Occurrences of hydrogen bonding organic solvents in molecular crystals." *Chem. Commun. (Cambridge)*, 605–606.
- Padmanabhan, S., Suresh, S., and Vijayan, M. (1995). "DL-Proline monohydrate." *Acta Crystallogr., Sect. C: Cryst. Struct. Commun.* **51**, 2098–2100.
- Rietveld, H. M. (1969). "A profile refinement method for nuclear and magnetic structures." *J. Appl. Crystallogr.* **2**, 65–71.
- Sheldrick, G. M. (2008). "A short history of SHELX." *Acta Crystallogr., Sect. A: Found. Crystallogr.* **64**, 112–122.

- Smith, G. S. and Snyder, R. L. (1979). " F_N : A criterion for rating powder diffraction patterns and evaluating the reliability of powder-pattern indexing," *J. Appl. Crystallogr.* **12**, 60–65.
- Thompson, P., Cox, D., and Hastings, J. B. (1987). "Rietveld refinement of Debye-Scherrer synchrotron X-ray data from Al_2O_3 ," *J. Appl. Crystallogr.* **20**, 79–83.
- Voet, D. and Voet, J. (1995). *Biochemistry*, 2nd ed. (Wiley, New York).
- Wallach, O. (1895). "Zur Kenntniss der terpene und der ätherischen oele," *Justus Liebigs Ann. Chem.* **286**, 90–143.
- Yin, Z. and Li, Z. (2006). "Conformational pseudo-polymorphs and hydrogen bonding of *m*-di-(pyrrole-2-carboxamide)-xylylene," *J. Mol. Struct.* **794**, 265–269.